Short Communication

Inhibition Behavior of Chitooligosaccharide Derivatives for Carbon Steel in 3.5% NaCl Solution

Fubin Ma[1,2,*], Yan Zhang[3], Hongjuan Wang[4], Weihua Li[1,2], Baorong Hou[1,2]

[1] Institute of Oceanology, Chinese Academy of Sciences, Qingdao 266071, China
[2] Open studio for marine Corrosion and Protection, Qingdao National Laboratory for Marine Science and Technology, Qingdao 266200, China
[3] China Electric Power Research Institute, Beijing 100192, China
[4] Sinopec PSTC Cangzhou Oil Transportion Department, Cangzhou, 061000, China
[*]E-mail: mfb281@163.com

Chitooligosacharide derivatives with different carboxymethylation degrees and grafting degrees of Schiff base were synthesized. Their inhibition property for carbon steel in 3.5% NaCl was tested by weight loss measurement, electrochemical measurements. The corrosion morphology of the specimens was examined by scanning electron microscope (SEM). The inhibition mechanism was analyzed by adsorption isotherm fitting and quantum chemical calculation. The results indicated that carboxymethylation improved the inhibition effect by increasing the compounds' solubility; while grafting of Schiff base increased the amount of effective active groups directly but had bad effect on the solubility. The molecules adsorbed on the carbon steel surface by physisorption and chemiadsorption according to Temkin adsorption isotherm and acted as a mixed type inhibitor.

1. INTRODUCTION

Chitosan is a kind of natural polymer which exists widely in nature and is usually extracted from shells of shrimps, crabs and insects and fungal cell walls. Due to its good film forming property, porosity and biological degradability, Chitosan plays an important role in many fields such as air pollution control, drinking water treatment and biodegradable material preparation and so on[1-4]. Its degradation product - chitooligosaccharide contains many –OH and $–NH_2$ groups which can be an environment-friendly corrosion inhibitor from the perspective of molecule structure[5-11]. Schiff base

(especially aromatic base Schiff base) containing -C=N- and -OH groups can form stable complex with iron ions thus suppressing corrosion reaction[12, 13]. Researches have found that aromatic base Schiff base has a good corrosion inhibition effect on the carbon steel in H_2S solution[14] and on zinc in H_2SO_4 solution[15]. Therefore, derivatives of Chitooligosaccharide Schiff base have a broad application prospects in corrosion protection field.

It has been reported that chitosan vanilina Schiff base generated from the reaction of chitosan and vanillina has better adsorbility but worse solubility in water[16, 17]. Therefore, the derivatives of chitosan and chitooligosaccharide are mainly used as corrosion inhibitors in acid media[18, 19]. However, one of the derivatives - carboxymethyl chitooligosaccharide vanillin Schiff base (CM-CSB) has good solubility[20-23]. There are –OH, -NH$_2$ and –COOH groups in the molecule which can generate complex with iron ions. However, its corrosion inhibition property and mechanism and the relationship between the property and molecular structure have been rarely reported. In the present paper, CM-CSB with different carboxymethylation degree and grafting degree of Schiff base are synthesized; then their corrosion inhibition property and mechanism and the relationship between the property and molecular structure are preliminary studied by weight loss and electrochemical measurements, corrosion morphology analysis, adsorption isotherm fitting and quantum chemical calculation.

2. EXPERIMENTAL

2.1 Synthesis of CM-CSB

The synthesis of CM-CSB includes two steps: Carboxymethylation of Chitooligosaccharide and preparation of Schiff base. The synthesis route is shown in Fig. 1.

(1) Carboxymethylation of Chitooligosaccharide

The Chitooligosaccharide (deacetylation degree: 91.5%, polymerization degree: 3-8, average molecular weight: 165) and NaOH with the mole ratio of 1:0.5, 1:1, 1:1.5 reacted in isopropanol solution for 2 hours at 45℃. Then chloroactic acid (its mole ratio with NaOH is 2-2.5:1) was added to the mixture and they react in water bath for 4 hours at 25℃ and 45℃. After rotary evaporation, multiple extraction and neutralization, carboxymethyl chitooligosaccharide with different carboxymethylation degree was obtained. At last, the carboxymethylation degree was measured by potentiometric titration.

(2) Preparation of Schiff base

Carboxymethyl chitooligosaccharide and vanillin with the mole ratio of 1:1 and 1:3 reacted in absolute ethyl alcohol and acetic acid for 10 hours in oil bath. After rotary evaporation, multiple extractions, CM-CSB compounds were obtained. The grafting degree was acquired by external standard method. The carboxymethylation degree and grafting degree of Schiff base of the products are listed in Table 1.

2.2 Materials and solution preparation

The specimens were the A3 carbon steel with chemical composition (wt %) of C (0.18%), Mn (0.55%), Si (0.3%), Cu (0.019%), S (0.034%), P (0.035%), Fe in balance. The test solutions were 3.5% NaCl solution which were prepared from reagent grade chemicals and double-distilled water with or without inhibitors.

2.3 Weight loss measurement
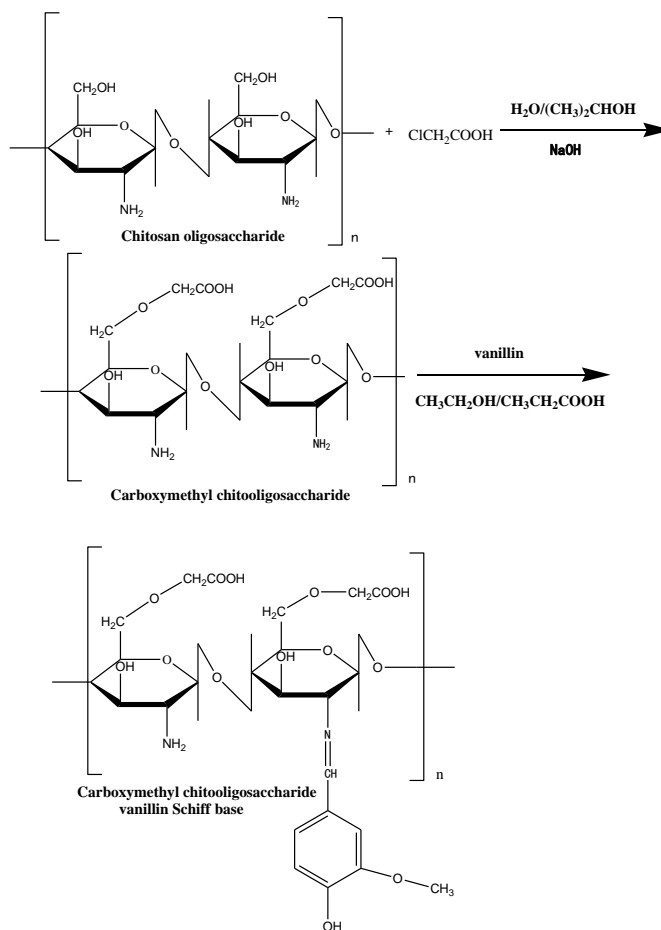
Figure 1. Synthesis route of CM-CSB

According to the standard JB/T 7901, *Uniform corrosion-Methods of laboratory immersion testing* was adopted in weight loss experiment. The A3 carbon steel sheets of 50.0mm×25.0mm×5.0mm with one φ4.0mm hole at one end were used. Before the test, they were abraded with a series of emery paper (grade 80, 240, 600, 800). Then they were cleaned with distilled water, degreased in acetone and ultrasonically cleaned in alcohol. After dried and weighed accurately, they were immersed in 350ml 3.5% NaCl solutions without/with different concentrations of inhibitors (100mg/l, 200mg/l, 400mg/l, 600mg/l, 800mg/l) for 15 days. Then they were weighed accurately by

analytical balance. The average weight loss data of each group for three parallel specimens was obtained. The inhibition efficiency (*IE%)* was calculated as follows:

$$IE\% = \frac{W_0 - W_1}{W_0} \times 100\%$$

Table 1. Carboxymethylation degree and grafting degree of Schiff base of CM-CSB

Number	Carboxymethylation degree / %	Grafting degree of Schiff base / %
A	28	24
B	42	24
C	61	24
D	28	27
E	42	30
F	61	41

2.4 Surface observation and analysis

The A3 carbon steel specimens (10.0 mm×10.0 mm ×10.0 mm) were polished to 2.5μm in the roughness. Then they were immersed in the NaCl solutions with different inhibitors with the concentration of 800mg/l. After 15 days, they were taken out, washed ultrasonically with absolute ethyl alcohol and acetone, and cleaned with distilled water. After drying, the specimens were directly observed by scanning electron microscope (KYKY2800B) with accelerating voltage of 25KV.

2.5 Electrochemical measurement

Electrochemical experiments were performed on the Parstat 2273 system (Princeton Applied Research) facilitated with a three-electrode system (shown as Fig.2). For the working electrode, except an exposed area of 10.0mm×10.0mm, the rest part was embedded in epoxy resin. The treatment of the working surface was the same as described in Section 2.3. The counter electrode was a platinum plate (15.0mm×15.0mm) and the reference electrode was a saturated KCl calomel electrode (SCE) coupled with a Luggin capillary.

The open circuit potential (OCP) measurements were conducted after 0.5 hour immersion in test solutions. When the OCP reached stable (the fluctuation was less than 2mV in 300 seconds), the electrochemical measurements could be performed. The potentiodynamic polarization curves were obtained within the range of OCP±250mV with the scan rate of 0.5mV/s. The electrochemical impedance spectra (EIS) were collected within the frequency range of 100kHz~10mHz using a 10mV sinusoidal potential perturbation. The data were obtained by the Powersuite software and fitted by the ZSimpWin software.

2.6 Quantum chemical calculation

For further study of the interaction between the adsorbed molecules and metal surface, molecular simulation and quantum chemical calculation were performed by Hyperchem 7.5 software. The structure of the molecular monomer was fully geometrically optimized in the way of PM3 in Semi-empirical way. Chemical indices such as the energy of the highest occupied molecular orbital (HOMO), the lowest unoccupied molecular orbital (LUMO), frontal orbital energy gap (ΔE=HOMO-LUMO), and dipole moment (μ) were calculated and compared.

3. RESULTS AND DISCUSSION

3.1 Weight loss measurement

The results of weight loss measurement for the specimens in 6 CM-CSB inhibitors at room temperature are shown in Fig.3.
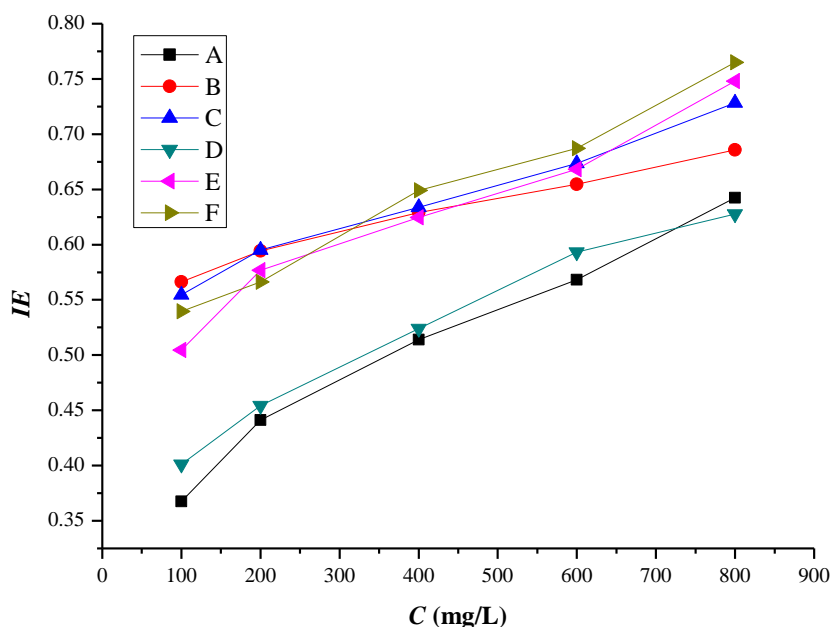
Figure 3. Relationship between inhibition efficiency and 6 CM-CSB inhibitors from 100mg/L to 800mg/L at room temperature

Fig. 3 shows that all the inhibitors have corrosion inhibition effect. Because all these inhibitors are derivatives of Chitosan polymer's degradation products. Due to the complex effect between their solubility and effective groups the IE is not higher than 80% when the concentration is no more than 800mg/L.The corrosion efficiency increases with the increase of concentration; when the concentration reaches 800mg/l, the efficiency is the highest. The efficiency of these inhibitors at 800mg/l is different in the order of F>E>C>B>A>D; for A, B and C, the inhibition effect tends to increase with the

carboxymethylation degree when the grafting degree is the same; for B and E, C and F, the efficiency increases with increasing grafting degree. For A and D, the efficiency decreases with the grafting degree when their carboxymethylation is low (only 28%); The inhibition effect of F is the best for its carboxymethylation and grafting degree are the highest; it has good solubility due to high carboxymethylation degree and has sufficient active adsorption groups (benzene and -C=N-) due to high grafting degree; therefore, the adsorption film is more compact and intact. After weight loss experiment, mahogany and viscous sediment appeared in the solution; they are probably chelate complex generated from the reaction of chitooligosaccharide derivatives with corrosion products (Fe^{2+} and Fe^{3+}).

3.2 Corrosion morphology analysis

A

B

C

D

E

F
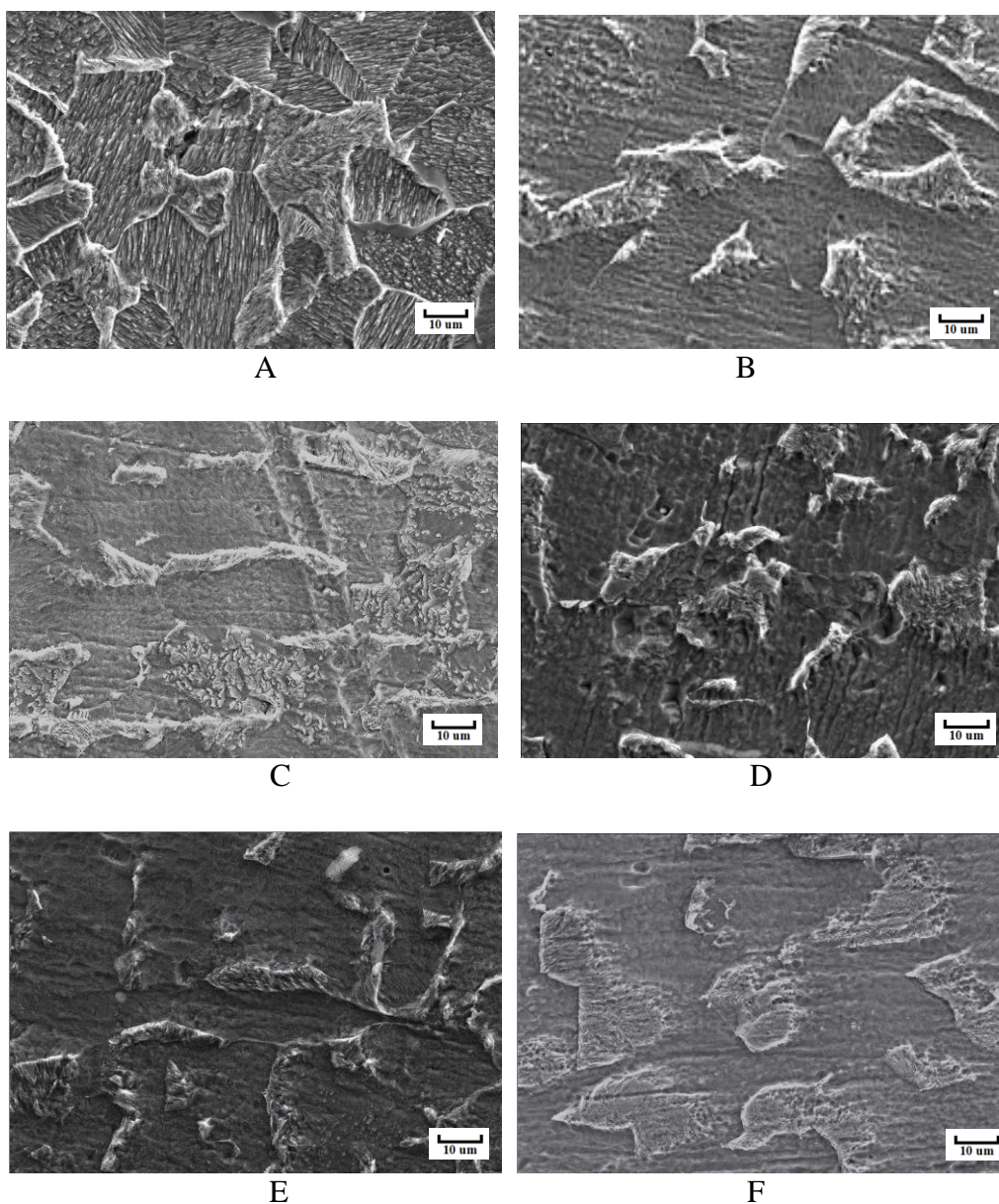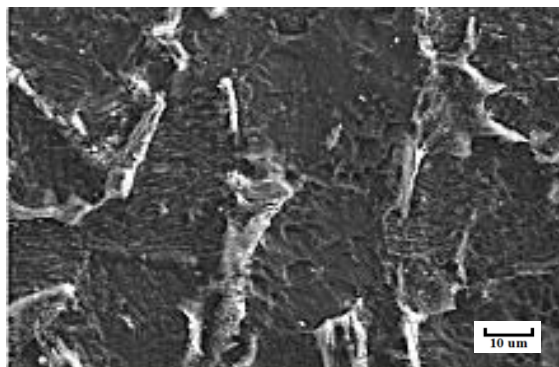
G

Figure 4. SEM micrographs of the specimens in the presence and absence of CM-CSBs

Corrosion morphology of the specimens in the solutions with 6 inhibitors (A-F) at 800mg/l and without inhibitor (G) is displayed by SEM as shown in Fig. 4. The corrosion inhibition effect is in the order of F>E>C>B>A>D. The specimen was strongly damaged with a lot of pits on the surface in the absence of inhibitor. The other specimens' surfaces had less pits and were less corroded. Corrosion status of D is more serious than that of A probably due to the difference of solubility; the film adopted on the surface has a weak bonding force with the substrate and easily falls off resulting in floccose sediment in the solution. The corrosion status of F is the lightest on which a few scratches could be seen probably because a protective adoption film forms on the surface thus alleviating corrosion reaction.

3.3 Potentiodynamic measurement

For better understanding on the inhibition mechanism, the inhibitor behavior of CM-CSB for carbon steel in 3.5% NaCl solution was further studied by potentiodynamic polarization. Depending on the carboxymethylation and grafting degree they are divided into 4 groups: A、 B and C, A and D, B and E, C and F. Fig. 5 presents the potentiodynamic polarization curves for carbon steel after 0.5 hour immersion in test solutions without and with inhibitors at 800mg/l. Table 2 shows the relevant electrochemical parameters obtained from the potentiodynamic polarization and IE is calculated based on the corrosion current. IE trend is similar with that of corrosion current. IE is slightly different from that of weight loss measurement because they are measured under different conditions. It can be seen that the corrosion current densities strongly decreased with the increase of carboxymethylation and grafting degree except A and D. The shapes of polarization curves are similar indicating that the inhibitors did not change the corrosion reaction mechanism. It can be ascribed to the surface structure change due to the inhibitor molecules adsorbing on the carbon steel surface. Fig. 5 a, c, d and Table 2 show that the corrosion potential shifts positively and the corrosion current density derived from extrapolation decreases sharply with the increase of carboxymethylation and grafting degree; the anodic Tafel slope remains nearly unchanged, while the cathodic Tafel slope tends to decrease with the increase of carboxymethylation and grafting degree. However, Fig b shows that the corrosion potential shifts negatively and current density increases in the presence of D compared with that of A; it maybe

caused by its low solubility. From the results above, it can be concluded that they are mixed type inhibitors. The molecules form protective film by adsorption on the carbon steel surface, which suppresses dissolution of carbon steel and diffusion of dissolved oxygen thus having corrosion inhibition effect. The formation of insoluble surface chelates blocks the adsorption of chloride effectively[24-27]. The solubility of the compounds improves with the increase of carboxymethylation which indirectly increases the number of effective groups such as benzene ring and -C=N-[28]. The increase of grafting degree directly provides more effective groups but can reduce the solubility to some extent; as a result, when the carboxymethylation reduces to a certain degree, the solubility of the compound becomes low thus affecting the corrosion inhibition. Just as some literatures have pointed out, solubility of Schiff base decreases with the increase of grafting degree[16, 20]. The results suggest that when the carboxymethylation is high enough, the inhibition effect increases with carboxymethylation and grafting degree.
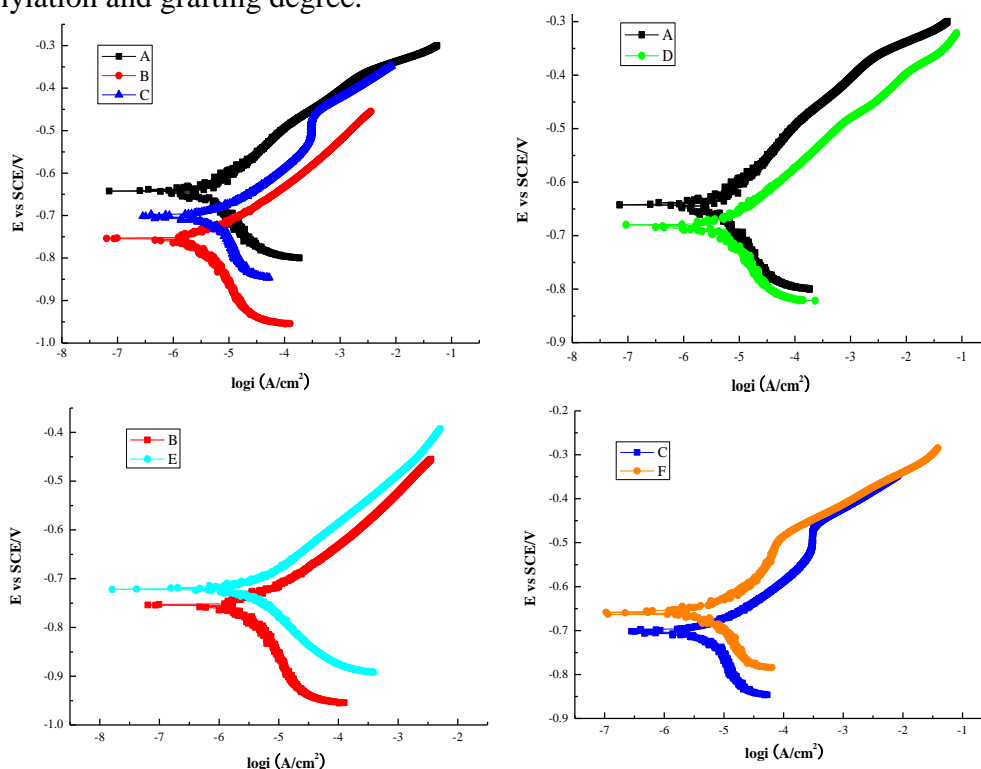
Figure 5. Polarization curves for the specimens in 3.5 % NaCl solution with 800mg/l CM-CSBs

Table 2. Polarization parameters for the specimens in 3.5 % NaCl solution without and with addition of CM-CSBs

inhibitor	E_{corr}/ mV	I_{corr}/uA·cm^{-2}	β_c/mV·dec^{-1}	β_a/mV·dec^{-1}	IE/%
blank	-723.8	14.24	363.8	82.1	/
A	-644.8	4.31	146.0	78.3	69.7
B	-749.5	3.58	214.0	71.8	74.9
C	-739.5	3.28	113.7	74.2	77.0
D	-740.4	4.85	221.6	76.0	65.9
E	-719.1	2.96	178.8	77.5	79.2
F	-660.4	2.18	94.2	73.5	84.7

3.4 Electrochemical impedance spectroscopy (EIS)

Fig. 6 shows the Nyquist plots for the carbon steel specimens in 3.5% NaCl solution with CM-CSBs at 800mg/l. From Fig. 6 a, c, and d we can observe that the diameters of the semi-circles increase with increasing carboxymethylation and grafting degree which indicate better inhibition effect. However, it is opposite in b which is probably caused by the solubility. These results agree with those obtained from potentiodynamic measurements. In addition, the impedance spectra don't present perfect semicircles, which can be attributed to the frequency dispersion[24, 25]. Base on the analysis, the Nyquist plots are composed of two distorted capacitive loops[24, 29-32]; the one at high frequency can be attributed to the capacitance of the Helmholtz plane on the surface corresponding to the charge transfer resistance (R_{ct}), while the one at low frequency is related to the adsorption film capacitance corresponding to the film resistance (R_f)[27, 31, 33]. Therefore, EIS results can be explained by the equivalent circuit model shown in Fig. 7. In the circuit, R_s, R_{ct} and R_f represent the solution resistance, the charge transfer resistance and the film resistance respectively. Considering the inhomogeneity at the solid/liquid interface, the double layer capacitance (C_{dl}) and the film capacitance (C_f) are replaced into the constant phase elements CPE_1 and CPE_2[26, 27, 33-35]. The values can be calculated by the following equation[36, 37]:

$$Z_{CPE}(\omega) = Y_0^{-1}(j\omega)^{-n}$$

Where Y_0 is the CPE constant, ω is the angular frequency (rad/s), $j^2 = -1$ and n is the CPE exponent. The fitted EIS parameters are listed in Table 3. It is apparent from Table 3 that in the presence of A, B and C, the C_{dl} and C_f values tend to decrease by increasing carboxymethylation degree while the R_{ct} and R_f values increase. The decrease in the capacitance values can be attributed to the decrease in the dielectic constant and/or the increase in the thickness of double electric layer due to the adsorption of the inhibitor molecule on the carbon steel surface[33, 36, 37]. The increase in R_{ct} suggests that the amount of inhibitor molecules adsorbed on the specimen surface increases consequently resulting in the decrease of active sites. IE can be calculated by the following formula:

$$IE\% = \frac{R_{ct} - R^o_{ct}}{R_{ct}} \times 100$$
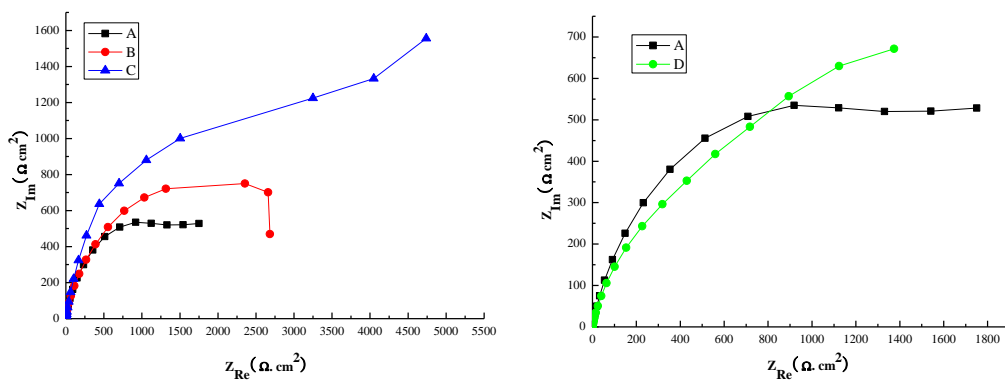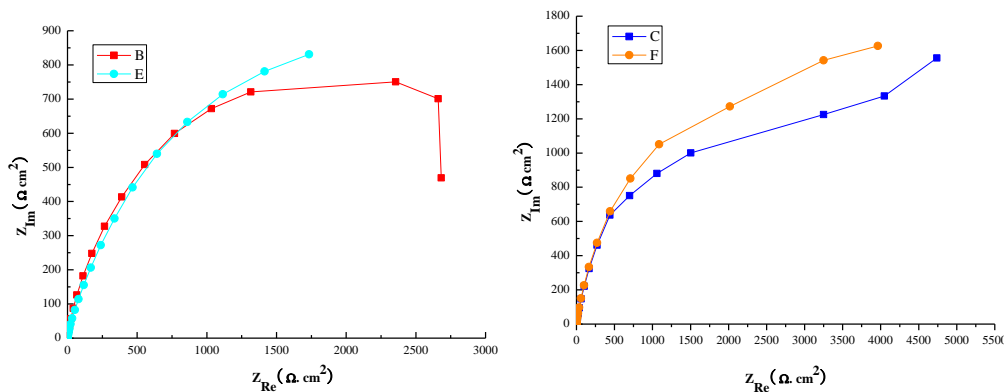
Figure 6. Nyquist plots for the specimens in 3.5 % NaCl solutions with 800mg/l CM-CSBs

The increase of R_f results from film formation by adsorbed inhibitor molecules and/or corrosion products on the carbon steel surface, thus increasing the pitting potential and suppressing the localized corrosion.
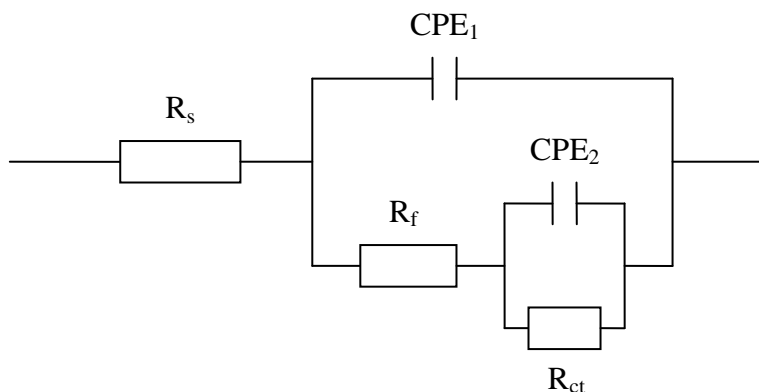
Figure 7. Equivalent circuit model

Table 3. EIS parameters of the specimens in 3.5 % NaCl solution with 800mg/l CM-CSBs

inhibitor	R_s /Ω cm^2	R_f /Ω cm^2	R_{ct} /Ω cm^2	C_{dl} /μF cm^{-2}	n_1	C_f /μF cm^{-2}	n_2	*IE/%*
blank	2.519	67.1	1102	524.6	0.76	286.3	0.89	/
A	2.210	155.8	4109	1263	0.92	224.5	0.92	73.2
B	2.087	160.3	4432	467.9	0.68	40.64	0.88	75.1
C	1.384	179.2	4604	432.4	0.74	35.67	0.90	76.1
D	3.509	108.0	3871	1406	0.56	473.9	0.75	71.5
E	2.115	205.4	5072	411.3	0.77	32.89	0.86	78.3
F	1.211	236.1	5892	382.1	0.82	25.14	0.76	81.3

From the perspective of molecular structure, the inhibitor molecule consists of polar groups composed of oxygen and nitrogen atoms which have high electronegativity and non-polar groups composed of carbon and hydrogen atoms; the polar groups can generate chelation adsorption with iron ions and form a protective film which changes the electric double layer and increases the

activation energy of ionization for metal atoms; whereas the non-polar groups directionally arrange on the metal surface and form a hydrophobic membrane thus producing inhibition effect[7, 12, 16, 20, 38]. The irregularity of A and D may be caused by their low solubility which can be proved by the flocculent sediment in the solution.

3.5 Adsorption isotherm

The effect of the corrosion inhibitor mainly depends on its adsorption ability and compactness of the film at metal/solution interface[39]. To obtain more information about the interaction, it is essential to investigate the mode of adsorption and the adsorption isotherm by experimental data. The values of surface coverageθat different concentrations calculated from weight loss measurement are used to fit adsorption isotherms including Freundlich, Langmuir, Temkin and Frumkin isotherm. The correlation coefficient (R^2) is used to compare the correlation between the surface coverage and the concentration. Temkin isotherm is found to be best fitted which can be expressed by the following equation:

$$\exp(f \cdot \theta) = K_{ads} \cdot C$$

where K_{ads} is the adsorption equilibrium constant, θ is the degree of surface coverage, C is the inhibitor concentration. f is the molecular interaction parameter which depends on the intermolecular interaction between the adsorption layer and heterogeneity of the surface[40]. If f is positive, mutual attraction of molecules occurs; while if f is negative, repulsion occurs. Compared with Langmuir adsorption, Temkin adsorption is an improved adsorption model. It is suitable for non ideal state adsorption on non-uniform surface. In this adsorption, there is an molecular interaction between the adsorbed molecules.
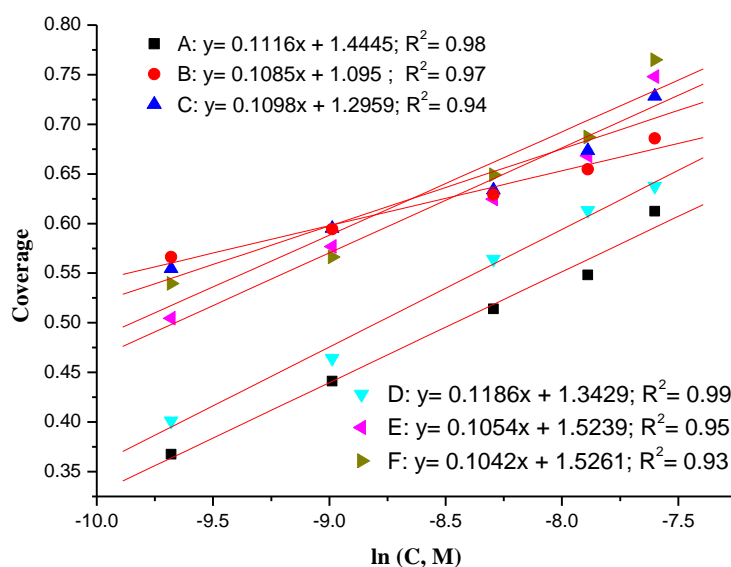
Figure 8. Adsorption isotherm fitting from weight loss measurement

Table 4. Absorption and thermodynamic parameters for CM-CSBs

inhibitor	K_{ads} (M^{-1})	ΔG^0_{ads} $(kJ \cdot mol^{-1})$	f
A	4.16×10^5	-41.59	8.98
B	2.41×10^4	-34.60	9.21
C	1.34×10^5	-38.81	9.11
D	8.28×10^4	-37.63	8.43
E	1.77×10^6	-45.13	9.44
F	2.29×10^6	-45.77	9.60

Plots of θ vs. lnC for six inhibitors are shown in Fig. 8. The linear relationship suggests that the adsorption on metal surface obeys Temkin adsorption isotherm. From the straight lines, the K_{ads} and f values are calculated. K_{ads} can be used to calculate the standard Gibbs free energy of adsorption ΔG by the following equation:

$$K_{ads} = \frac{1}{55.5} \exp(\frac{-\Delta G^0_{ads}}{RT})$$

where 55.5 is the molar concentration of water, R is the gas constant ($8.314 KJ^{-1}mol^{-1}$) and T is the absolute temperature (K). The thermodynamic parameters derived from Temkin adsorption isotherm for the compounds are given in Table 4. From the table we can see that the calculated K_{ads} values are more than 10^4 which indicate the formation of strong and stable adsorption layer on the metal surface[41]. Values of standard Gibbs free energy of adsorption around -20kJ·mol^{-1} or lower indicate physisorption, while those around or higher than -40 kJ·mol^{-1} indicate chemisorption. The calculated ΔG values range from -34.60 to -45.77 kJ·mol^{-1} which suggest the adsorption of compounds occurs both by chemisorption and physisorption[42, 43], but with increasing grafting degree of Schiff base the adsorption mainly depends on chemisorption and is a spontaneous process[44-46]. Moreover, the value of f is positive which implies that the interaction between the molecules causes an increase of the adsorption energy with increasing surface coverage. The trend of f is basically the same as the trend of grafting degree of Schiff base. All above results indicate that the inhibitors adsorb on the metal surface by chemisorption and physisorption in the form of Temkin adsorption. The effective adsorption groups are probably the benzene ring and -C=N- groups. Also there is an molecular interaction between the adsorbed molecules. The interaction becomes stronger with increasing grafting degree of Schiff base.

3.6 Quantum chemical calculation

The effectiveness of an inhibitor depends on its spatial molecular structure and electronic structure[47, 48]. For further understanding the interactions between the inhibitor molecules and the carbon steel surface, quantum chemical calculation is performed[49]. Frontier molecular orbital theory is useful in predicting the adsorption centers. The energy of the highest occupied molecular orbital (HOMO) E_{HOMO} is related with the electron donating ability of the molecule[50, 51]. High values of E_{HOMO} indicate a tendency for the molecule to donate electrons to appropriate acceptor molecules. The

energy of the lowest unoccupied molecular orbital - E_{LUMO} indicates the ability of accepting electrons to molecule[52-54]. The optimized molecular monomer structure, the highest occupied molecular orbital (HOMO) and the lowest unoccupied molecular orbital (LUMO) is respectively shown in Fig. 9 and the calculated quantum chemical parameters are displayed in table 5. For HOMO of the molecule, it can be observed that the benzene ring and -C=N- have large electric density, while for the LUMO, -C-C- and –C=N- has large electron density; it suggested that the adsorption centre is on benzene ring and -C=N-. That is, the molecules can directly adsorb on the steel surface on the basis of donor-acceptor interactions between the electrons of the benzene ring, -C=N- and the vacant d-orbital of iron atoms[55, 56]. The more grafting degree of Schiff base, the more effective groups. Therefore, it can be concluded that the corrosion inhibition increases with the grafting degree which is consistent with the weight loss and electrochemical measurements. Moreover, it can be concluded that carboxymethylation don't play a direct role in inhibition effect, but improves the solubility of the inhibitors increasing the number of effective groups indirectly.

CM-CSB monomer   HOMO   LUMO
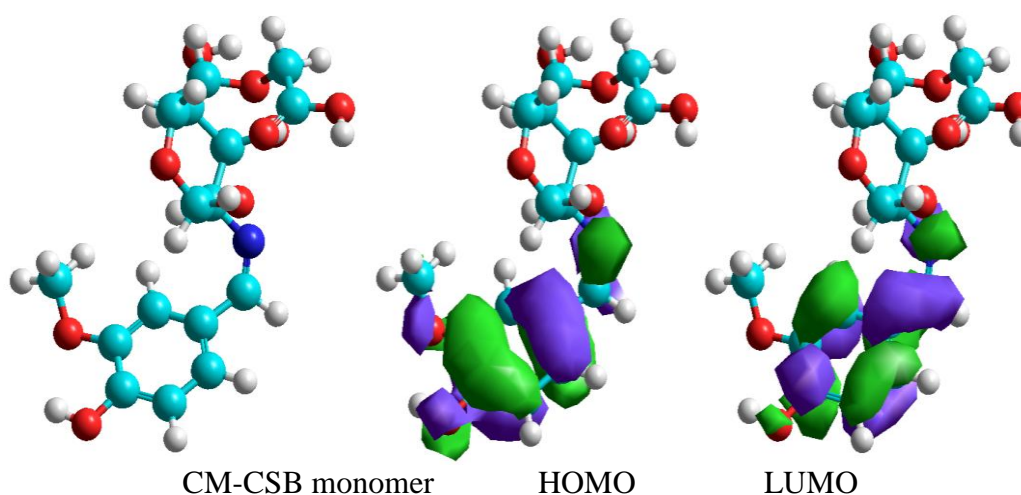
Figure 9. Molecular structure and frontier molecule orbital density distribution CM-CSB monomer

Table 5. Calculated quantum chemical parameters of CM-CSB monomer

Parameter	E_{HOMO} (eV)	E_{LUMO} (eV)	ΔE (eV)	μ/debye
CM-CSB	-9.07	-0.29	8.78	3.07

4. CONCLUSIONS

(1) The compounds are mixed-typed inhibitors and their corrosion inhibition effect increases with concentrations in different degrees.

(2) When the concentration is high and the carboxylation of the inhibitor is low, corrosion inhibition effect reduces with increasing grafting degree; however, when the carboxylation is also high, inhibition effect increases with increasing grafting degree.

(3) Carboxylation and grafting have different effect on corrosion inhibition. Grafting can directly provide more effective groups but have a bad effect on the solubility whereas carboxylation can improve the solubility which is necessary for a good inhibitor.

(4) These compounds adsorb on the carbon steel surface in the form of non ideal state adsorption; the adsorption obeys the Temkin adsorption isotherm with combined actions of physisorption and chemiadsorption. There   is an molecular interaction between the adsorbed molecules.

References

1. M. Rinaudo, *Prog. Polym. Sci.*, 31 (2006) 603.
2. S.-K. Kim, N. Rajapakse, *Carbohyd. Polym.*, 62 (2005) 357.
3. B. Krajewska, *Enzyme Microb. Tech.*, 35 (2004) 126.
4. N. Yusof, A. Wee, L.Y. Lim, E. Khor, *J. Biomed. Mater. Res.* A, 66A (2003) 224.
5. F. Ma, W. Li, H. Tian, Q. Kong, B. Hou, *Int. J. Electrochem. Sci.*, 7 (2012) 10909.
6. J. Brugnerotto, J. Lizardi, F.M. Goycoolea, W. Arguelles-Monal, Desbrieres, M. Rinaudo, *Polymer,* 42 (2001) 3569.
7. S. Banerjee, V. Srivastava, M.M. Singh, *Corros. Sci.*, 59 (2012) 35.
8. Y. Yan, W. Li, L. Cai, B. Hou, *Electrochim. Acta,* 53 (2008) 5953.
9. L. Feng, H. Yang, F. Wang, *Electrochim. Acta,* 58 (2011) 427.
10. J. Zhang, X.L. Gong, H.H. Yu, M. Du, *Corros. Sci.*, 53 (2011) 3324.
11. X. Zhou, H. Yang, F. Wang, *Corros. Sci.,* 54 (2012) 193.
12. H.D. Leçe, K.C. Emregül, O. Atakol, *Corros. Sci.*, 50 (2008) 1460.
13. S. Şafak, B. Duran, A. Yurt, G. Türkoğlu, *Corros. Sci.,* 54 (2012) 251.
14. R.K. Vagapov, L. V. Frolova, Y.I. Kuzenetsov, *Prot. Met.*, 38 (2002) 27.
15. Y.K. Agrawal, J.D. Talati, M.D. Shah, M.N. Desai, N.K. Shah, *Corros. Sci.,* 46 (2004) 633.
16. R. Jayakumar, D. Menon, K. Manzoor, S.V. Nair, H. Tamura, *Carbohyd. Polym.*, 82 (2010) 227.
17. A. Einbu, S. Naess, A. Elgsaeter, K. Varum, *Biomacromolecules,* 5 (2004) 2048.
18. A.M. Fekry, R.R. Mohamed, *Electrochim. Acta,* 55 (2010) 1933.
19. S. Cheng, S. Chen, T. Liu, X. Chang, Y. Yin, *Mater. Lett.*, 61 (2007) 3276.
20. T. Sun, P. Xu, *Eur. Polym. J.,* 39 (2003) 189.
21. H. Kweon, H.C. Ha, I. C. Um, Y.H. Park, *J. Appl. Polym. Sci.,* 80 (2001) 928.
22. S.S. Zeng,S.J. Wang, M. Xiao, D.M. Han, Y.Z. Meng, *Carbohyd. Polym.* 86 (2011) 1260.
23. Y.-W. Cho, J. Jang, C. Park, S.-W. Ko, *Biomacromolecules,* 1 (2000) 609.
24. L. Valek, S. Martinez, D. Mikulić, I. Brnardić, *Corros. Sci.*, 50 (2008) 2705.
25. A. Balbo, C. Chiavari, C. Martini, C. Monticelli, *Corros. Sci.*, 59 (2012) 204.
26. M.B. Valcarce, M. Vázquez, *Electrochim. Acta,* 53 (2008) 5007.
27. M.B. Valcarce, M. Vazquez, *Mater. Chem. Phys.*, 115 (2009) 313.
28. J.R. Xavier, S. Nanjundan, N. Rajendran, *Ind. Eng. Chem. Res.*, 51 (2012) 30.
29. X. Zhou, H. Yang, F. Wang, *Electrochim. Acta,* 56 (2011) 4268.
30. M. Sánchez, J. Gregori, M.C. Alonso, J.J. Garcia-Jareño, H. Takenouti, V. Vicente, *Electrochim. Acta,* 52 (2007) 7634.

31. M. Sánchez, J. Gregori, M.C. Alonso, J.J. Garcia-Jareño, V. Vicente, *Electrochim. Acta,* 52 (2006) 47.
32. C. Gabrielli, S. Joiret, M. Keddam, N. Portail, P. Rousseau, V. Vivier, *Electrochim. Acta,* 53 (2008) 7539.
33. H.E. Jamil, A. Shriri, R. Boulif, C. Bastosc, M.F. Montemor, M.G.S. Ferreira, *Electrochim. Acta,* 49 (2004) 2753.
34. F. Mansfeld, *Electrochim. Acta,* 35 (1990) 1533.
35. Y.S. Choi, J.J. Shim, J.G. Kim, *Mater. Sci. Eng., A*385 (2004) 148 .
36. X. Wang, H. Yang, F. Wang, *Corros. Sci*., 52 (2010) 1268.
37. M. Salasi, T. Shahrabi, E. Roayaei, M. Aliofkhazraei, *Mater. Chem. Phys*., 104 (2007) 183.
38. N.H. Helal, W.A. Badawy, *Electrochim. Acta,* 56 (2011) 6581.
39. M. Lebrini, M. Lagrenée, H. Vezin, M. Traisnel, F. Bentiss, *Corros. Sci*., 49 (2007) 2254.
40. A. Yurt, G. Bereket, A. Kivrak, A. Balaban, B. Erk, *J. Appl. Electrochem.* 35 (2005) 1025.
41. K.F. Khaled, K. Babić-Samardžija, N. Hackerman, *Electrochim. Acta,* 50 (2005) 2515.
42. D.J. Lavrich, S.M. Wetterer, S.L. Bernasek, G. Scoles, *J. Phys. Chem*. B, 102 (1998) 3456.
43. S.M. Wetterer, D.J. Lavrich, T. Cummings, S.L. Bernasek, G. Scoles, *J. Phys. Chem*. B, 102 (1998) 9266.
44. M. Bouklah, B. Hammouti, M. Lagrenée, F. Bentiss, *Corros. Sci*., 48 (2006) 2831.
45. W. Li, Q. He, C. Pei, B. Hou, *Electrochim. Acta,* 52 (2007) 6386.
46. M.S. Morad, *Corros. Sci.,* 50 (2008) 436.
47. A.Y. Musa, R.T.T. Jalgham, A.B. Mohamad, *Corros. Sci*., 56 (2012) 176.
48. S. Xia, M. Qiu, L. Yu, F. Liu, H. Zhao, *Corros. Sci.,* 50 (2008) 2021.
49. M. Finšgar, A. Lesar, A. Kokalj, I. Milošev, *Electrochim. Acta,* 53 (2008) 8287.
50. K.F. Khaled, *Electrochim. Acta,* 53 (2008) 3484.
51. G. Gece, *Corros. Sci.,* 50 (2008) 2981.
52. E. Machnikova, K.H. Whitmire, N. Hackerman, *Electrochim. Acta,* 53 (2008) 6024.
53. I.B. Obot, N.O. Obi-Egbedi, *Corros. Sci*., 52 (2010) 198.
54. H. Ashassi-Sorkhabi, B. Shaabani, D. Seifzadeh, *Electrochim. Acta* 50 (2005) 3446.
55. F. Ma, W. Li, H. Tian, B. Hou, *Int. J. Electrochem. Sci*., 10 (2015) 5862.
56. A. Lalitha, S. Ramesh, S. Rajeswari, *Electrochim. Acta,* 51 (2005) 47.